Applied Physics A (2023) 129:94
https://doi.org/10.1007/s00339-023-06393-8

Applied Physics A
Materials Science & Processing

Investigation of gate-engineered heterostructure tunnel field effect transistor as a label-free biosensor: a compact study

Rittik Ghosh[1] · **Ananya Karmakar**[2] · **Priyanka Saha**[3]

Received: 13 September 2022 / Accepted: 4 January 2023 / Published online: 10 January 2023

Abstract
In this article, the authors have articulated DC as well as transient response of a dielectric modulated gate-engineered heterostructure tunnel field effect transistor (GE-HTFET)-based biosensor for label-free detection. A low (direct) bandgap material, indium arsenide (InAs) has been selectively used in the source region to achieve improved band-to-band tunneling of carriers in the tunnel FET. The extended gate architecture is incorporated to stabilize the biomolecules in the nano-cavity aiding significant boost in ON current sensitivity. Using SILVACO ATLAS TCAD tool, the sensitivity of the biosensor is evaluated considering two important parameters possessed by bio-targets, i.e. dielectric constant (k) and charge density (N). A thorough analysis has been performed to show the impact of variation of dielectric constants and charge density of biomolecules over transfer characteristics of the device. ON current level (Ion) is eventually extracted which is considered here as the suitable sensing parameter of the device. Transient response to detect the settling time of Ion is also demonstrated here in presence of both positively and negatively charged bio-species with varying values of dielectric constant. Then ON current sensitivity is extracted accordingly for different locations of biomolecules within the nano-gap. Finally, an extensive comparative analysis of the present structure in terms of ON current sensitivity is shown to justify its sensing ability as compared to recently reported device structures.

Keywords Dual metal · Gate-engineered · Heterostructure · Tunnel FET · Dielectric modulation · Biomolecules · Sensitivity

1 Introduction

Recent research advances in the field of microbiology have led to an upsurge in the detection of nano-biomolecules with utmost precision. Biomolecules like APTES, biotin–streptavidin, gelatin, DNA, different kinds of bacteria and viruses need efficient identification for understanding any kind of behavioral change inside the living cell. Therefore, a highly sensitive, reliable, higher lifetime, low power and low-cost biosensor is the need of the hour. In recent advances, field effect transistors (FET)-based biosensors have proven as excellent biosensing devices and can be used effectively as an alternative to costly conventional sensors. Apart from being highly sensitive, reliable, fast and cost-effective, FET (MOSFET, TFET)-based biosensors have an added advantage for their compatibility with complementary metal oxide semiconductor (CMOS) technology. This makes them suitable for on-chip integration as the downscaling of devices continue to follow Moore's law. The dielectric modulation approach towards biomolecules identification using FET (MOSFET, TFET)-based biosensors is emerging as a major researcher interest. In FET (MOSFET, TFET)-based biosensors, the functionalized (nano-gap) dielectric layer under gate metal has been incorporated with specific receptors where the desired biomolecules can be captured selectively giving rise to gating effect. The gating effect can be converted into readable signals like the change in

✉ Rittik Ghosh
rittik.ghosh2021@vitstudent.ac.in

Ananya Karmakar
ananya26m@gmail.com

Priyanka Saha
priorient06@gmail.com

[1] Department of Micro and Nano Electronics, VIT, Vellore, India

[2] Department of Electronic Science, University of Calcutta, Kolkata, India

[3] Department of Electronics and Communication Engineering, IIIT Kota, Rajasthan, India

drain characteristics, threshold voltage characteristics or channel conductance. Different biomolecules have different dielectric constants (k), like streptavidin ($k=2.1$), biotin ($k=2.63$), APTES ($k=3.57$), gluten ($k=5$), zenin ($k=7$), keratin ($k=10$), gelatin ($k=12$) [1, 2]. MOSFETs have their unique electrical properties that have been a spectacle for the researchers over the years. But its limitations to short channel effects (SCEs) and its restrictions over subthreshold swing (SS) to 60 mV/dec at room temperature (limiting the scaling of supply voltage) affects its sensing operations [3]. Tunnel field effect transistors (TFETs) have proven to overcome the above-mentioned limitations and is ideal for low-power VLSI applications mainly because of their lowered OFF current (I_{off}) [4]. Tunnel FETs have their unique property of band-to-band tunnelling (BTBT) which arises due to their p-i-n (N-type) or n-i-p (P-type) device doping profile. The mode of conduction of charge carriers in the channel differs from that of MOSFETs which essentially follows thermionic emission phenomenon. Due to these, tunnel FETs can achieve sub 60 mV/dec SS, thereby reducing its power consumption and making it suitable for low power applications. However, even though TFETs have steep switching behavior and fast response time [5], they have unacceptably low ON current (I_{on}) in comparison to MOSFETs [4]. In conventional tunnel FETs, gate controllability determines the tunnelling rate at the source–channel interface.

A positive gate voltage of an N-type TFET bends the bands at the source–channel interface and drain current is realized. Applying a negative gate voltage on an N-type TFET will bend the bands at the drain–channel interface giving rise to drain current as well. This limitation of conventional TFET is called ambipolar conduction that limits it for use in digital circuit design. Asymmetrical doping profile of the source and the drain (heavily doped source and lightly doped drain) reduces ambipolar current at the drain–channel interface [6]. Hence, different structures have been introduced to improve the I_{on} of TFETs [7–9]. In recent times, different label-free TFET-based biosensors have been investigated taking sensitivity parameter into consideration for benchmarking like SiGe source and pocket-doped channel [10], dielectric-modulated TFET-based biosensor [11], N + pocket-doped vertical TFET-based dielectric-modulated biosensor [12], dielectric-modulated dual channel trench gate TFET-based biosensor [13], back-gate bias and front-gate engineering DMTFET-based biosensors [14]. It has been investigated that these models are either having low sensitivity or complex fabrication process. To overcome the above limitations, in this work, III–V gate-engineered heterostructure tunnel FET biosensor is proposed. Heterostructure architecture in tunnel FET aids in higher tunnelling rate at the tunnelling interface due to the presence of bandgap modulating material at the tunnelling interface. Smaller bandgap at tunnelling junction leads to much reduced tunnel width, thus, ensuring higher overlap of conduction band with valence band. Heterojunction TFET, therefore, exhibits higher Ion as compared to conventional TFET owing to greater band bending at the tunnelling interface. This Ion in turn being a parameter of sensitivity, thereby, improves the ON state current sensitivity of the device significantly, and hence suitable for sensing applications. However, hetero TFETs has one major limitation which restricts its widespread applications and need rigorous research study to overcome it. Tripathy et al. [15] discuss the key drawback of the heterojunction TFETs of high Ioff as compared to conventional silicon-based TFETs. Hence, apart from source material engineering, device structural engineering is implemented as alternate solution to enhance Ion and reduce Ioff of TFET device. In this regard, different device architectures such as vertically grown TFET, L-shaped/U-shaped TFET, and source pocket engineered TFET have been explored and reported in literature [15]. The enclosed architecture as shown in Fig. 1a exhibits improved ON current sensitivity, reduced leakage current, higher Ion/Ioff ratio, steeper SS due to the extension of tunneling and auxiliary gates of the proposed biosensor. Moreover, easier fabrication steps involved in InAs/Si process as described in Fig. 1b [16] make the proposed biosensor suitable for commercial use.

Due to the compatibility with low power applications, such emerging lab-on-chip heterostructure-based biosensors are widely used in biomedical and healthcare industries, DNA detection, forensic industries, environmental monitoring for efficiently sensing biomolecules. Furthermore, Bhowmick et al. also reported heterostructure TFET as an excellent candidate for detection of COVID-19 virus [17].

The focus of this work is to perform the DC and transient response analysis for III–V gate-engineered heterostructure TFET (GE-HTFET) biosensor for neutral, positively, and negatively charged biomolecules.

2 Device structure and simulation framework

The 3D and 2D schematic diagram of the nano-gap functionalized GE-HTFET structure for biosensing application along with the dimensions is shown in Fig. 1a. Indium arsenide (InAs) has been used in the P + type source material and silicon (Si) has been used in the rest of the intrinsic channel and N + type drain region creating a heterostructure/heterojunction. Beside indium gallium arsenide (InGaAs) [1], InAs is also a direct bandgap semiconductor, having smaller electron effective mass (m_e^*) causing its mobility of charge carriers to be as much as 20 times higher than that of Si which has a relatively high m_e^*[18] enhancing the I_{on}. Also, the bandgap of InAs (Eg = 0.354 eV) is much lower than the bandgap of

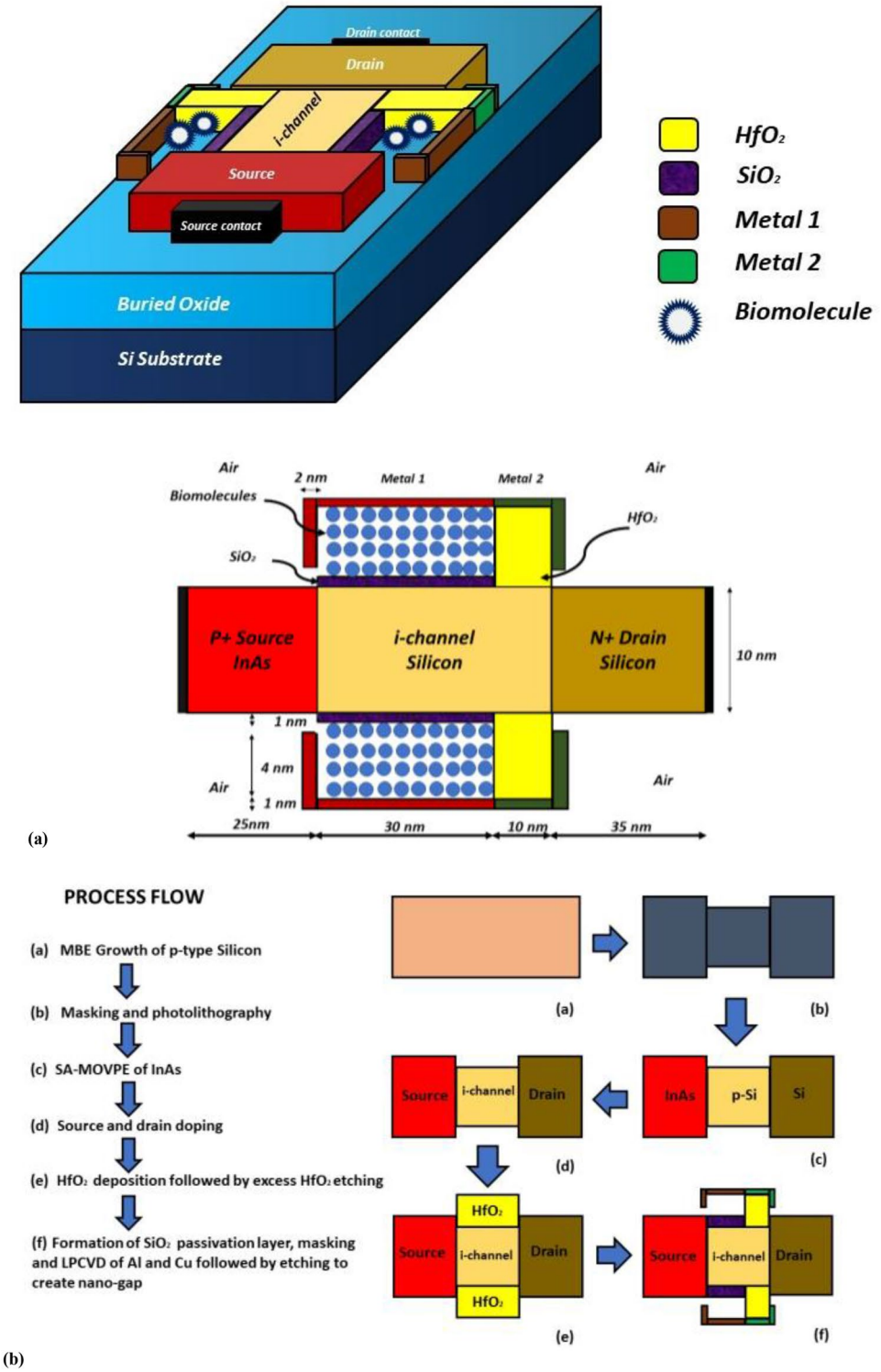

Fig. 1 **a** 3D and 2D schematic diagram of the nano-gap functionalized proposed GE-HTFET biosensor in presence of biomolecules **b** potential fabrication process flow of GE-HTFET

Si (Eg = 1.1 eV) which creates a straddling band alignment structure upon the formation of InAs/Si heterostructure. It helps in the improvement of tunnelling at the source–channel interface by reducing the tunnelling width owing to sharp band bending [1]. InAs and Si has a lattice mismatch of approximately 11.6%. The fabrication process of InAs/Si using selective-area metal–organic vapor epitaxy (SA-MOVPE) has been reported in [17]. Figure 1b shows the potential fabrication process flow of proposed GE-HTFET. The gate architecture is engineered with extensions of two different metal, tunnelling gate (aluminium = Φ_{m1} = 3.8 eV) and auxiliary (copper = Φ_{m2} = 4.8 eV). The extended

tunnelling gate provides enhanced gate controllability resulting in higher BTBT rate and the extended auxillary gate controls the thermionic emission [1]. In our present work, we have included the concept of gate engineering technique which employs two different work functions for tunnelling and auxiliary gate metal. Across the source/channel interface, lower work function of gate material ($\Phi_{m1} = 3.8$ eV) leads to lower the barrier across the tunnelling junction so that tunnelling of carriers is facilitated under the tunnelling gate. This, in turn, enhances the I_{on} of the device. Simultaneous controlling of the I_{off} of the device is contributed by applying high work function ($\Phi_{m2} = 4.8$ eV) gate material of auxiliary gate to enlarge the barrier across the drain/channel junction. Suppressing the inherent ambipolar conduction of TFET device is also possible by adopting this novel hetero gate material. Thus, this gate-engineered TFET structure has dual benefits of high I_{on} (due to low work function gate metal across source/channel tunnelling junction) and low I_{off} (due to high work function gate metal across drain/channel interface), thereby improving the overall I_{on}/I_{off} ratio considerably. For biosensing operations, it is taken into consideration that the nano-gap is empty at $k = 1$ (air) and completely filled with biomolecules with different values of dielectric constant k. The gate controllability over the tunnelling junction is weak at $k = 1$, i.e. when the nano-gap is empty. To overcome this, a lower work function ($\Phi_{m1} = 3.8$ eV) metal has been carefully used over the nano-gap (source–channel region). When the nano-gap is filled ($k = 12$) with biomolecules, it will improve the electric field at the interface and cause sharp band bending at the source–channel interface increasing the band-to-band tunnelling (BTBT) rate, thereby improving I_{on}. The gate metal work function is chosen such that tunnelling of charge carriers will take place only when the nano-gap is filled with biomolecules so that an accurate change in the sensing parameter can be observed. To facilitate this, a higher work function ($\Phi_{m2} = 4.8$ eV) metal is used over HfO_2 dielectric material. Precisely, tunnelling gate is the controller of SS whereas auxiliary gate is the controller of the leakage current [1]. However, the consequences of using a high work function metal as the tunnelling gate will not facilitate proper band bending which will restrict tunnelling [19]. In this paper, GE-HTFET, the channel length is 40 nm for analysis. The height of passivation layer (SiO_2) is 1 nm and HfO_2 is selected as a gate dielectric. The height of silicon channel is 10 nm while the nano-gap length is 30 nm. The P-type InAs source is doped with 1×10^{20} cm^{-3}, N-type Si drain is doped with 1×10^{18} cm^{-3}. The intrinsic Si channel is doped with 1×10^{15} cm^{-3}. The results obtained in Fig. 7b shows that the proposed GE-HTFET has peak sensitivity for 4 nm EG [20]. It is a fact that single cavity biosensors are effective in comparison to dual cavity biosensors as single cavity biosensors cause sharp band bending in the source–channel interface at $k = 1$(air) and $k = 12$(filled), and provides enhanced coverage of the nano-gap when compared to dual cavity biosensors. In dual cavity biosensors, the split nano-gap design reduces the coverage area of the nano-gap, thereby reducing the change in effective capacitance between gate and channel [1]. SILVACO ATLAS TCAD tool [21] is used to simulate the proposed GE-HTFET. Tunnelling is pointed at the source–channel interface using a non-local BTBT model which is based on WKB approximation. To introduce the mobility degradation effect, CONMOB and FLDMOB models have been applied. We have also used drift diffusion model, Shockley–Read–Hall (SRH) model, and Auger model to include the effect of recombination and generation for electrons and holes. For further accuracy of band-to-band tunnelling, Fermi–Dirac statistics and band gap narrowing (BGN) models are included. The device models and parameters of P-type InAs/Si TFET are calibrated by comparing with the experimental data as reported in [22]. Figure 2 shows the calibration of simulation results with experimental data.

3 Results and discussion

The presence of biomolecules inside the nano-gap with its increasing dielectric constant (k) results in vertical electric field at the source–channel tunnelling interface shown in Fig. 3a [1]. Due to the amplified gate coupling, highest electric field is observed for gelatin biomolecule ($k = 12$). This results in enhanced channel penetration and significant shift in surface potential as shown in Fig. 3b. From Fig. 4, it is observed that the extended tunnelling gate provides sharp band bending at the source–channel interface in the presence of biomolecules inside the nano-gap whereas the extended

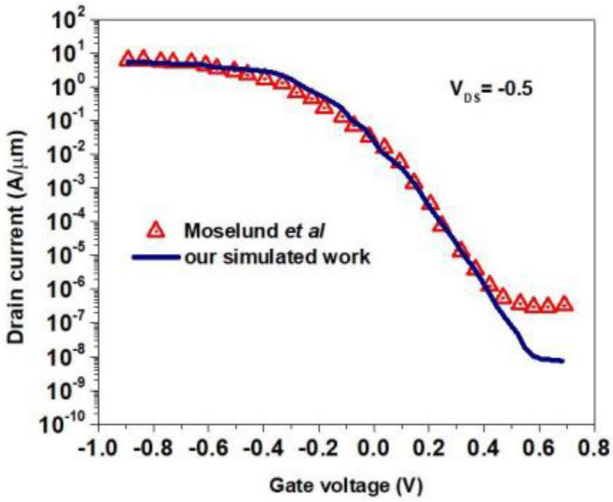

Fig. 2 Calibration of transfer characteristics of P-type InAs/Si TFET for the proposed simulation model against the experimental data [22]

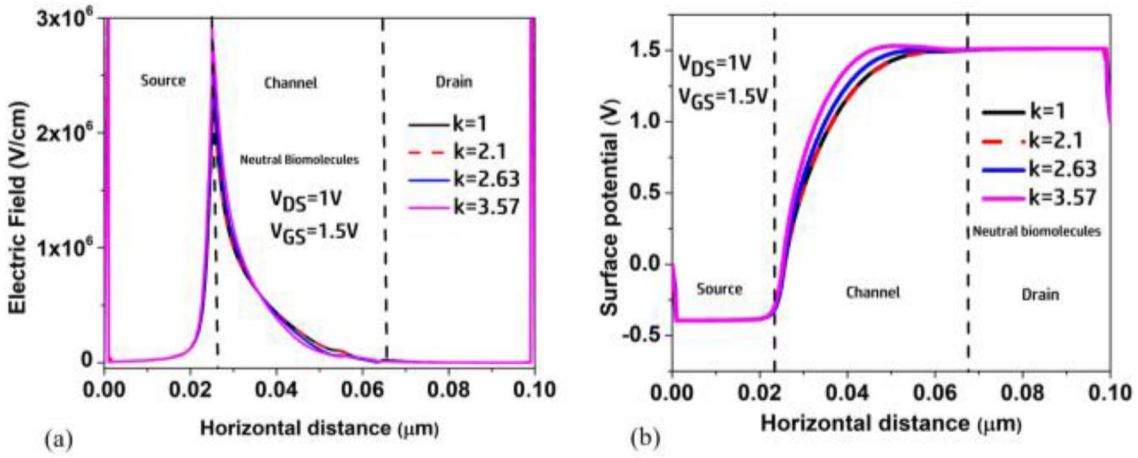

Fig. 3 **a** Electric field and **b** surface potential profiles of the proposed GE-HTFET-based biosensor in the presence of neutral biomolecules with different dielectric constant (*k*)

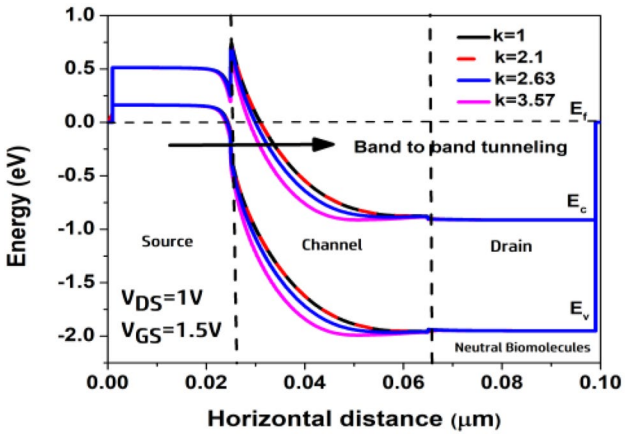

Fig. 4 Energy band profile of the proposed GE-HTFET in the presence of different neutral biomolecules with different dielectric constant (*k*)

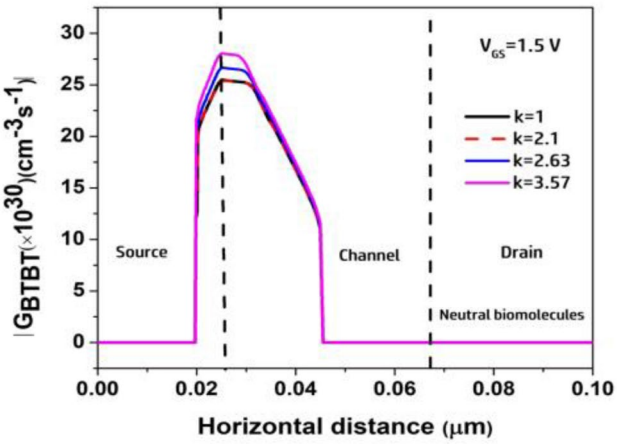

Fig. 5 BTBT generation rate of the proposed GE-HTFET-based biosensor in the presence of neutral biomolecules with different dielectric constant (*k*)

auxiliary gate controls the I_{off} by pulling the band upwards at the drain–channel interface.

Thereby, extended gate (EG) architecture facilitates increased BTBT generation rate (G_{BTBT}) resulting in higher I_{on} values.

$$G_{BTBT} = AE^{\sigma}\exp\left(\frac{-B}{E}\right) \tag{1}$$

where A depends on effective mass of an electron, B depends on the tunnelling probability, and σ denotes transition constant. The maximum tunnelling in TFET structures happens at the maximum value of BTBT rate, G_{BTBT}. To determine the tunnelling probability in TFET structures, Wentzel–Kramer–Brillouin (WKB) approximation is taken into consideration [13], T_{WKB} and is given by:

$$T_{WKB} \approx \exp\left(\frac{-4\lambda\sqrt{2m^*}\sqrt{E_g^3}}{3q\hbar\left(E_g + \Delta\phi\right)}\right) \tag{2}$$

where λ denotes screening tunnelling width, m^* represents effective mass of an electron, E_g bandgap energy, Δϕ represents the energy range over which tunnelling can occur. From (1) it is observed mathematically that with the increase in the dielectric constant of biomolecules in the nano-gap, the band bending sharpens because of high of electric field. From (2) we can conclude mathematically that when the dielectric constant of biomolecules increases, the tunnelling width reduces and T_{WKB} increases which will raise the I_{on} [23]. Figure 5 highlights the increase in BTBT generation.

Rate profile for the proposed GE-HTFET biosensor with increase in the dielectric constant of biomolecules (k) inside the nano-gap. The use of non-local BTBT model in SILVACO ATLAS TCAD aids in treating the BTBT phenomenon as a classical generation process. Electrons (not holes) drive significantly high BTBT generation rate when biomolecule is present inside the nano-gap [23]. From the DC transfer characteristics shown in Fig. 6, a change of approximately ten orders of magnitude in the I_{on} is observed when the dielectric constant of biomolecules (k) change from $k=1$ (air-filled nano-gap) to $k=12$ (gelatin-filled nano-gap). Low I_{on} values of 10^{-17} to 10^{-18} A are observed for the proposed GE-HTFET biosensor with air-filled nano-gap [13, 24]. For such FET-based biosensors, the signal-to-noise ratio (SNR) would be limited during practical applications [25].

For a dual metal MOSFET (DM MOSFET) biosensor, I_{off} is significantly high than the DM TFET biosensor. Low I_{off} results in low static power dissipation in DM TFET biosensor.

3.1 Sensitivity of ON current (S_{on})

The most important criteria to determine the performance of a

$$S_{on} = \left| \frac{I_{ON}(biomolecule)}{I_{ON}(air)} \right| \tag{3}$$

biosensor is its sensitivity. From (3), the sensitivity of ON current is evaluated by the relative ratio of I_{on} in the presence and absence of biomolecules inside the nano-gap. The reason behind particularly selecting I_{on} as the sensing parameter lies in the fact that TFET I_{on} mainly depends on BTBT rate. Parameters like SS, threshold voltage shift (ΔV_{th}), I_{on}/I_{off} ratio largely drive sensitivity of a biosensor [1]. Asymmetrically doped source and drain helps in achieving improved sensitivity of the biosensor [23]. From Fig. 7a, it is observed that the proposed GE-HTFET exhibits appreciably high change in S_{on} of approximately six orders of magnitude when the dielectric constant of neutral biomolecules (k) change from $k=1$ (air-filled nano-gap) to $k=12$ (gelatin-filled nano-gap). The proposed device exhibits maximum S_{on} of 7.96×10^{9} when the nano-gap is filled with neutral gelatin ($k=12$) biomolecules. Figure 7b provides understanding of S_{on} of the proposed GE-HTFET with different extended gate

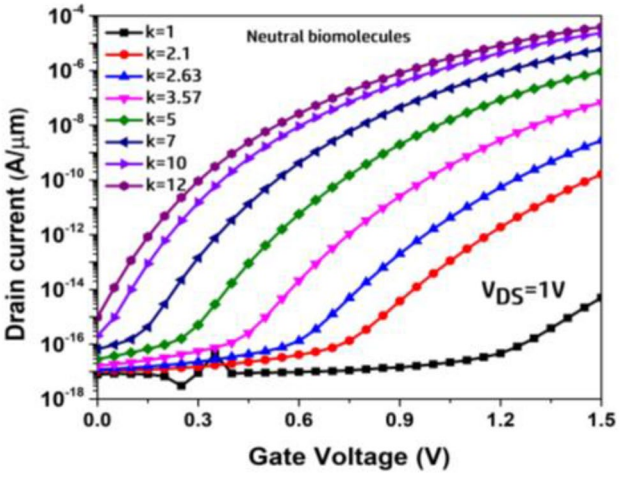

Fig. 6 Transfer characteristics of the proposed GE-HTFET-based biosensor in the presence of neutral biomolecules with different dielectric constant (k)

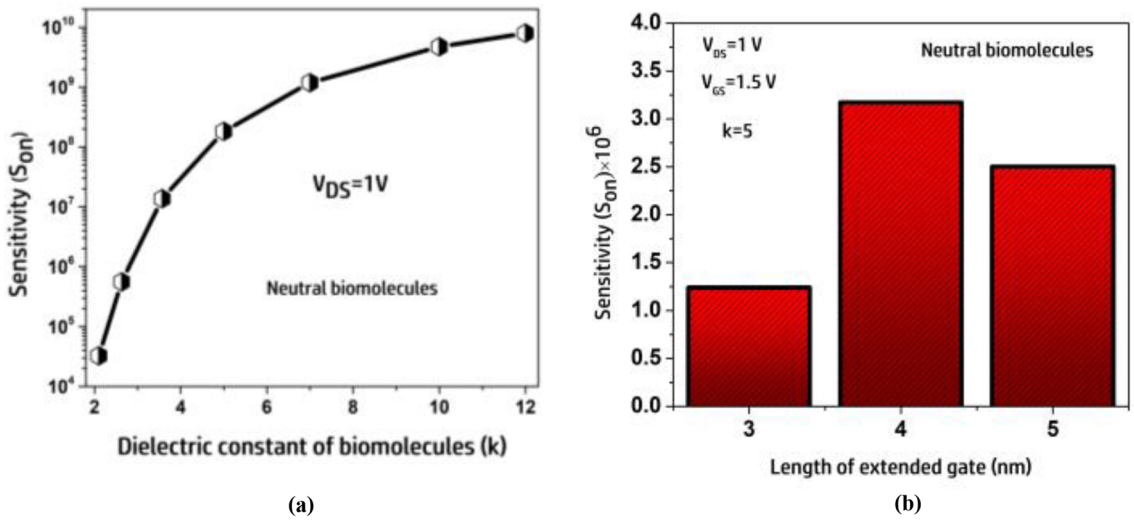

Fig. 7 **a** ON current sensitivity (S_{on}) of the proposed GE-HTFET-based biosensor in the presence of different neutral biomolecules with different dielectric constant (k), **b** ON current sensitivity (S_{on}) of the proposed GE-HTFET-based biosensor for different extended gate lengths at $k=5$

lengths for gluten biomolecule ($k=5$) inside the nano-gap. It is evident that the proposed biosensor provides optimum S_{on} for 4 nm extended gate length.

3.2 Impact of charged biomolecules

Furthermore, some biomolecules like DNA gets ionized upon binding with the receptors. It is important to analyze the performance of a biosensor in presence of neutral as well as charged biomolecules. The voltage balance equation for MOSFET is given by

$$V_{GS} = \psi_s + \phi_{ms} - \left(\frac{q\left({}^{+}_{-} N \right)}{C_{eff}} \right) \tag{4}$$

where ψ_s is surface potential, N is charged biomolecules, C_{eff} is the effective capacitance per unit area, ϕ_{ms} is the metal–semiconductor work function. (4) reflects, for fixed V_{GS} and fixed dielectric constant of biomolecules, when + N is increased then there will be a subsequent increase in ψ_s, thereby increasing the sensitivity of the device [18]. This is due to the increase in $\frac{+qN}{C_{eff}}$ factor at the SiO_2 boundary which depletes the lightly doped P-type channel at much lower gate voltage, leading to sharp band bending at the source–channel interface [13], as shown in Fig. 8a consequently reducing the threshold voltage and increasing the I_{on} of the device. Similarly, when -N is increased, then ψ_s lowers decreasing the sensitivity of the device as shown in Fig. 8b. This is due to the increase in $\frac{-qN}{C_{eff}}$ factor at the SiO_2 boundary, which increases threshold voltage. This will increase the tunnelling width at the source–channel interface, thereby decreasing the tunnelling rate [26] and subsequently decreasing the I_{on}.

In this paper, the charge of biomolecules is varied from $N = \text{to } N = {}^{+}_{-} 2 \times 10^{12} Ccm^{-2}$.

3.3 Transient response

Also, transient analysis is performed on the biosensor to exploit the settling time of I_{on} in presence of biomolecules inside the nano-gap [24]. Subsequently, analysis of transient response for sensitivity as well as selectivity is performed for the proposed GE-HTFET biosensor to get detailed biosensing outputs. The proposed biosensor is simulated for transient response with gate voltage of 1.5 V, step time (T_{step}) of 10^{-12} s (s), ramp time (T_{ramp}) of 10^{-6} s, and stop time (T_{stop}) of 10^{-1} s. Figure 9 shows that with the increase in dielectric constant of biomolecules (k) inside the nano-gap, I_{on} increases in the stable state (DC state). It is observed that for varying biomolecules, I_{on} achieves stable state at distinct settling times [28, 29]. For gelatin biomolecule ($k=12$) inside the nano-gap, I_{on} takes shortest settling time to reach the stable state. When the nano-gap is air filled, longest settling time to reach the stable state is observed. Thereby, the magnitude of G_{BTBT} is a driving factor behind settling time [29]. G_{BTBT} is low for biomolecules with low dielectric constants (k) reducing I_{on}, resulting in longer settling time. For biomolecules with higher dielectric constants (k), G_{BTBT} is higher, increasing I_{on}, resulting in shorter settling time. From the analysis, it is evident that gate controllability over the source–channel tunnelling interface remains unchanged from DC analysis. As stated in the DC analysis, biomolecules inside the nano-gap are sensed by relative ratio of I_{on} during the presence and absence of biomolecules inside the nano-gap [30–34] as evident in (3). A transient response approach to determine the S_{on} of the proposed GE-HTFET biosensor for different biomolecules at specific time stamps is shown in Fig. 10a. S_{on} is evaluated for streptavidin ($k=2.1$) to gelatin ($k=12$) neutral biomolecules at 10^{-9} s,

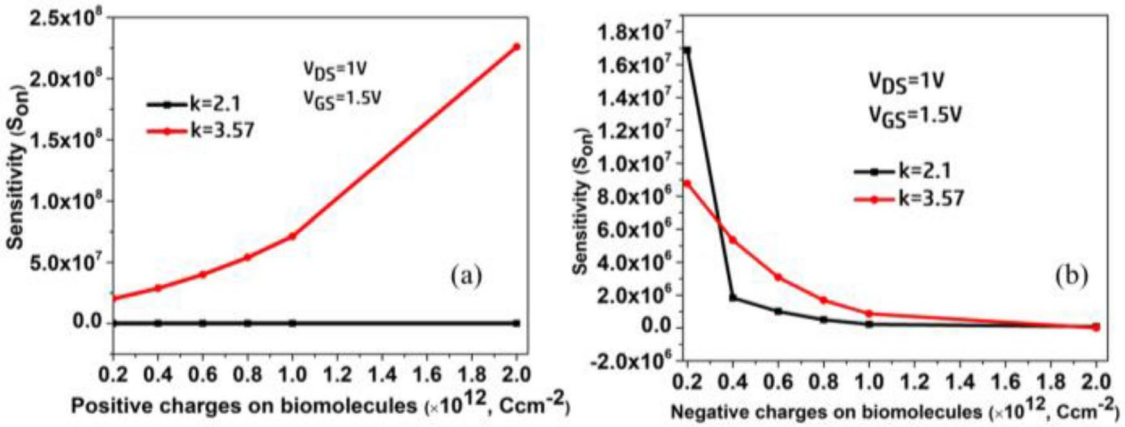

Fig. 8 ON current sensitivity Son of the proposed GE-HTFET in presence of ionized biomolecules with **a** positive charges **b** negative charges

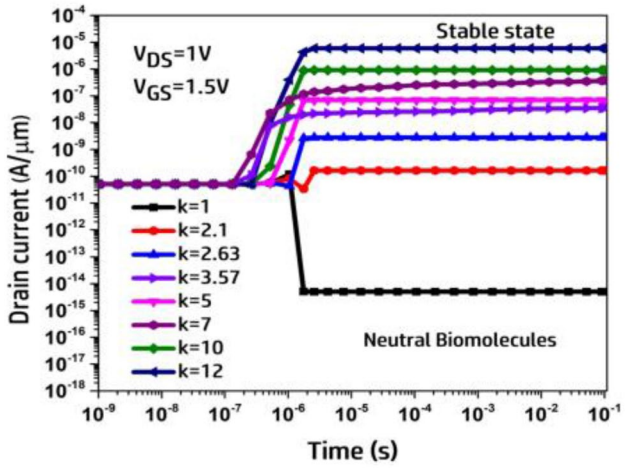

Fig. 9 Transient response of ON current (I_{on}) of the proposed GE-HTFET-based biosensor in the presence of different neutral biomolecules with different dielectric constant (k)

10^{-6} s, 10^{-3} s time stamps. Similar to DC analysis, maximum S_{on} (7.96×10^{9}) is achieved for gelatin ($k=12$). It is observed that gelatin biomolecule achieves a change of approximately ten orders of magnitude while streptavidin attains a change of approximately four orders of magnitude. Apart from sensitivity, selectivity of a FET-based biosensor to be able to distinguish biomolecules is an important performance metric [35]. Selectivity (ΔS) of a FET-based biosensor is evaluated by the relative ratio of I_{on} for biomolecule 1 over biomolecule 2, given by:

$$\Delta S = \left| \frac{I_{ON}(biomolecule1) - I_{ON}(biomolecule2)}{I_{ON}(biomolecule2)} \right| \quad (5)$$

Transient response approach can be implemented for realizing greater values of selectivity (ΔS) to distinguish specific biomolecules in presence of different other biomolecules [23]. Figure 10b shows the selectivity of the proposed GE-HTFET biosensor for the reported biomolecules at 10^{-9} s, 10^{-6} s, 10^{-3} s time stamps. ΔS_1, ΔS_2, ΔS_3, ΔS_4, ΔS_5, ΔS_6 represent selectivity of biotin over streptavidin, APTES over biotin, gluten over APTES, zenin over gluten, keratin over zenin, gelatin over keratin, respectively. Maximum selectivity $(\Delta S_1) \sim 10^2$ has been reported for biotin ($k=2.63$) over streptavidin ($k=2.1$). Minimum selectivity $\Delta S_1 \sim 10^0$ is observed for gelatin ($k=12$) over keratin ($k=10$). Selectivity (ΔS) of the proposed device reduces as dielectric constants of the biomolecules (k) inside the nano-gap increase. Similar to the DC analysis, from voltage balance Eq. (4), as + N increases, Ψs increases resulting in increase in I_{on} and Ψs reduces when -N is increased resulting in decrease in I_{on}. From Fig. 11a–d, it can be observed that I_{on} increases (decreases) significantly for positively (negatively) charged biomolecules inside the nano-gap. The highest positively (negatively) charged biomolecule takes the shortest (longest) settling time to reach the stable state.

The tunnelling width decreases (increases) with the increase in positive (negative) charges on the biomolecules, thereby increasing (reducing) G_{BTBT} [26]. Similar to the DC analysis, the charge of biomolecules is varied from $N = \pm 2\times10^{11} Ccm^{-2}$ to $N = \pm 2\times10^{12} Ccm^{-2}$. In practical applications, the agglomeration of biomolecules inside a

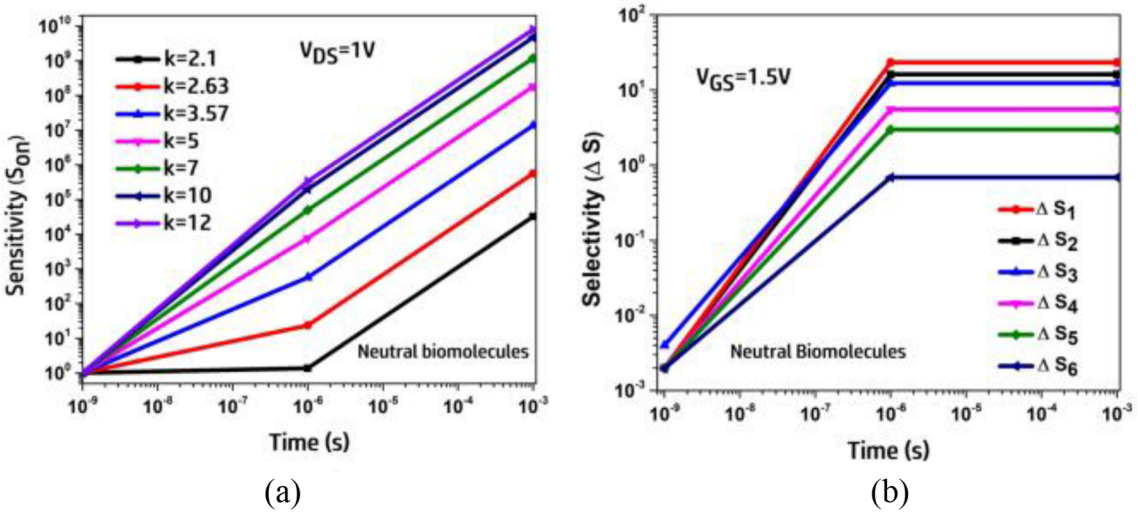

Fig. 10 **a** ON current sensitivity (S_{on}) with time. **b** Selectivity ΔS with time for the proposed GE-HTFET in the presence of different neutral biomolecule with different dielectric constant (k)

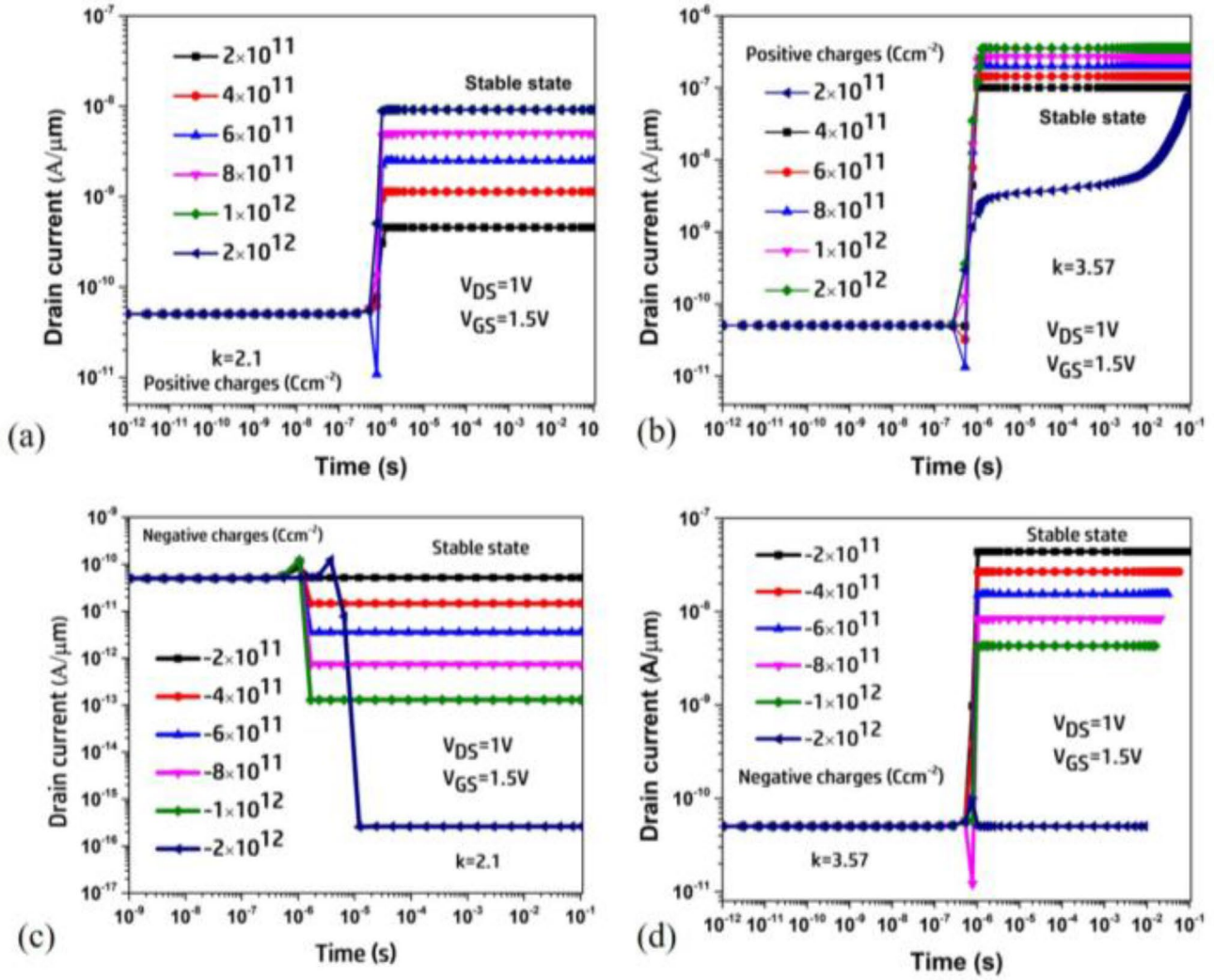

Fig. 11 Transient response of ON current due to positive charges at **a** $k=2.1$ **b** $k=3.57$ and negative charges at **c** $k=2.1$ **d** $k=3.57$ of the proposed GE-HTFET-based biosensor

functionalised nano-gap can be quite complex from the usual simulation setup [31, 36–40]. This has been analysed with a 50% fill-in factor (γ) with APTES ($k=3.57$) biomolecule in Fig. 12. Figure 12a shows four different locations of biomolecule inside the nano-gap with $\gamma=50\%$. From Fig. 12b, the transfer characteristics for four different cases of biomolecule locations inside the nano-gap, case A, case B, case C, case D are observed. Highest value of I_{on} is achieved for case A when $\gamma=50\%$ biomolecules accumulated over the source–channel tunnelling interface. The gate controllability over the tunnelling interface narrows the tunnelling width resulting in higher I_{on} value. It is noted that the I_{on} value achieved for case A with $\gamma=50\%$ is approximately equal to $\gamma=100\%$. For case B and case C, $\gamma=50\%$ biomolecules are accumulated at the centre and near the drain–channel interface, respectively, away from the tunnelling interface. Therefore, gate controllability over the tunnelling junction decreases, decreasing its ability to narrow the tunnelling width, lowering I_{on} value. For case D, $\gamma=50\%$ biomolecules are present throughout the source–channel tunnelling interface till the drain–channel interface. But lower gate control in case D is reported in comparison to case A and $\gamma=100\%$ due to the presence of air above the accumulated biomolecules throughout the nano-gap. Figure 12c shows the transient response approach for case A, case B, case C, case D. As stated in the DC analysis, maximum value of I_{on} is achieved for case A. Lower values of I_{on} are observed for case B and case C when $\gamma=50\%$ biomolecules are accumulated near the centre and drain–channel interface, respectively. Shortest settling time is observed in case A due to enhanced G_{BTBT} and longest settling time is observed in case C due to low G_{BTBT}. Figure 12d highlights the transient response approach to determine the S_{on} for case A, case B, case C, case D 10^{-9} s, 10^{-6} s, 10^{-3} s time stamps. For case A,

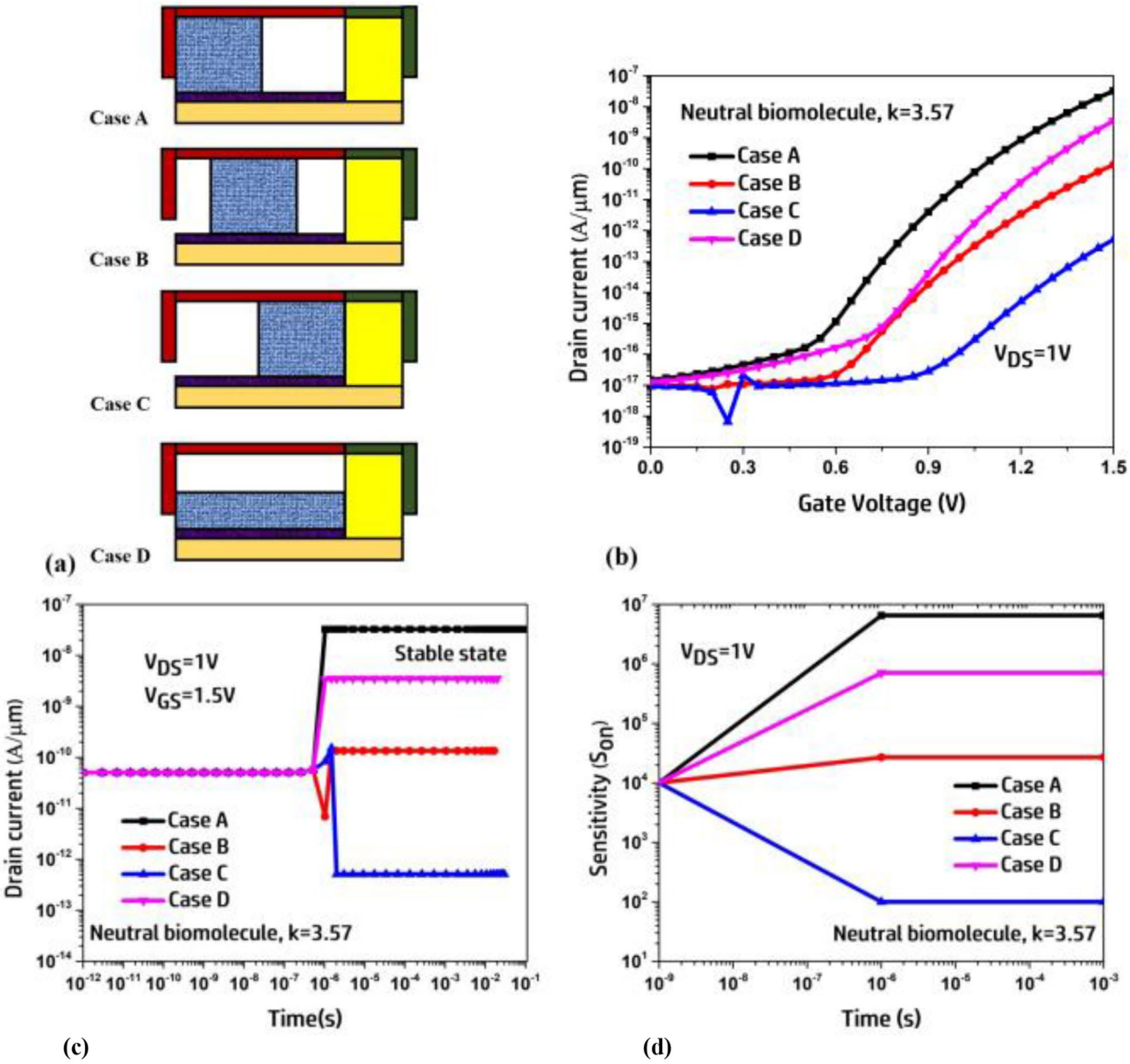

Fig. 12 **a** Schematic illustration of the proposed GE-HTFET biosensor for four different positions of APTES biomolecule with γ = 50%, case A, case B, case C, case D. **b** Transfer characteristics for four different cases. **c** Transient response of four different cases. **d** ON current sensitivity (S_{on}) with time

γ = 50% biomolecules are accumulated over the tunnelling interface that reduces the tunnelling width due to increased gate controllability over the tunnelling interface. As a result, I_{on} increases significantly, thereby increasing S_{on}. For case B and case C, γ = 50% biomolecules are accumulated at the centre and near to the drain-channel interface respectively which is away from the tunnelling interface. Therefore, I_{on} reduces because of reduction of gate controllability over the tunnelling width, thereby reducing S_{on}. For case D, low S_{on} is observed when compared to case A and γ = 100% due to presence of air in the vertical direction inside the nano-gap. Therefore, it is observed that when the biomolecules are accumulated near the tunnelling interface, S_{on} increases and TFET behaves as a better biosensor. S_{on} reduces when the biomolecules are shifted away from the tunnelling interface. Hence, S_{on} is maximum for case A followed by case D and considerably low for case B and case C [39, 40]. Furthermore, for analysing the transient response, a realistic approach of detecting streptavidin ($k = 2.1$) using transient has been shown in Fig. 13 for γ = 100%. In Fig. 13a (i) 4.2 nm thick APTES biomolecule is used as oxide binding protein (ii) 3.8 nm thick biotin is stacked over 4.2 nm thick

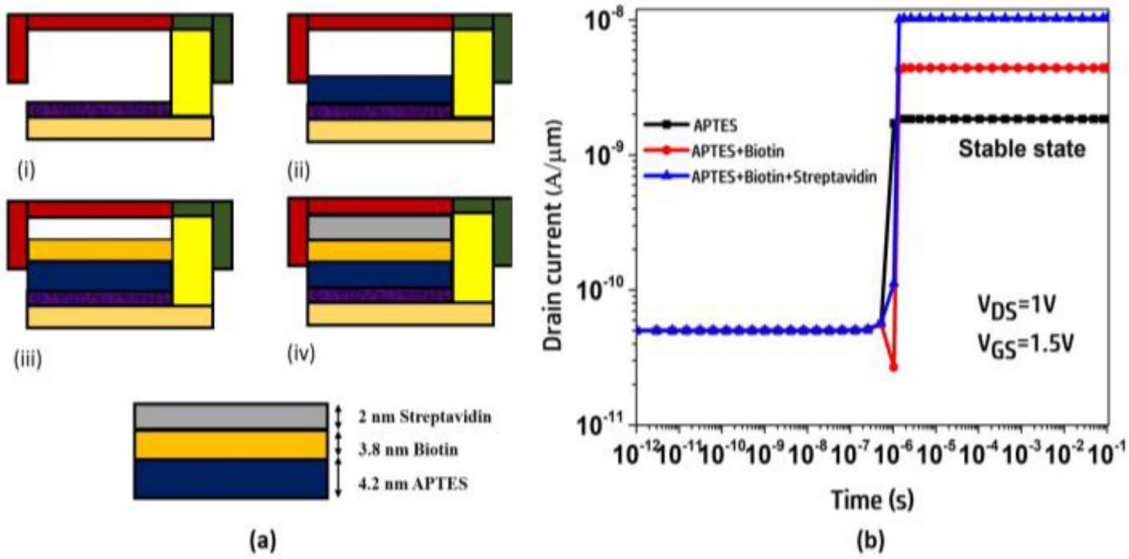

Fig. 13 **a** Schematic illustration of the proposed GE-HTFET biosensor (i) air-filled nano-gap (ii) APTES-filled nano-gap (iii) APTES + biotin-filled nano-gap (iv) APTES + biotin + streptavidin-filled nano-gap. **b** Transient response of APTES, APTES + biotin, APTES + biotin + streptavidin stacked nano-gap

APTES (iii) 2 nm thick streptavidin (biotarget) is stacked over 3.8 nm thick biotin and 4.2 nm thick APTES inside the nano-gap. From Fig. 13b, maximum I_{on} is observed for accumulation of streptavidin over biotin over APTES (streptavidin + biotin + APTES). Thus, transient response can be successfully used as a tool for achieving realistic approach for biosensing operations [23]. Performance benchmarking of the proposed GE-HTFET biosensor with the previous FET-based biosensors is shown in Table 1 in terms of ON current sensitivity (S_{on}). It can be seen that our proposed GE-HTFET biosensor provides a much better S_{on} of 7.96×10^9 compared to the FET-based biosensors available in the literature.

The results obtained in Fig. 14 well describe the contribution of GE-HTFET in boosting the ON state current sensitivity of the proposed device as compared to existing TFET structures (e.g., Ge source DMDG TFET, SC-DM0EG TFET).

Table 1 Performance benchmarking of published FET-based biosensors considering ON current sensitivity (S_{ON})

Sl. no.	TFET-based biosensors	ON state current sensitivity (S_{ON})
1	Lateral DM HTFET (L_{gap} = 20 nm, L_{Ch} = 42 nm, k = 2.1) [40]	10
2	Single pocket DM TFET (L_{gap} = 20 nm, L_{Ch} = 42 nm, k = 2.1) [40]	40
3	SiGe source DM PNPN TFET (L_{gap} = 20 nm, L_{Ch} = 42 nm, k = 2.1) [10]	4×10^3
4	Double gate (DG) TFET (L_{gap} = 30 nm, L_{gate} = 40 nm, k = 12) [11]	1.05×10^2
5	DM NT-TFET (L_{gap} = 50 nm, L_{gate} = 50 nm, k = 10) (V_{GS} = 0.6 V) [26]	$\sim 8 \times 10^5$
6	Ge source DM NT-TFET (L_{gap} = 50 nm, L_{gate} = 50 nm, k = 10) [26]	6×10^5
7	InAs source DM NT-TFET (L_{gap} = 50 nm, L_{gate} = 50 nm, k = 10) [26]	8×10^5
8	Charge plasma based DM NT-TFET (L_{gap} = 10 nm, 50 nm, L_{gate} = 20 nm & 11 nm, k = 8) [41]	~ 50
9	Diagonal tunneling based DM NT-TFET (L_{gap} = 95 nm, L_{gate} = 50 nm + 45 nm, k = 10) [11]	$\sim 10^{10}$
10	Dual channel trench gate biosensor (L_{gap} = 90 nm, L_{gate} = ~ 90 nm, k = 12) [42]	7×10^{12}
11	N + pocket-doped vertical TFET (L_{gap} = 20 nm & 30 nm, L_{gate} = 40 nm & 30 nm, k = 10) [11]	3×10^5
12	Core–shell junctionless NT-TFET (L_{gap} = 100 nm, L_{gate} = 50 nm, k = 8, 50% filled) [43]	$\sim 2 \times 10^2$
13	Doping less DLDGTFET ((L = 50 nm, Lgs = 3 nm, Lgd = 15 nm, k = 12, cavity length 30 nm) [44]	1×10^{10}
14	Dual metal GE-HTFET (LGAP = 30 nm, LGATE = 40 nm, HGAP = 10 nm, k = 12) (present work)	7.96×10^9

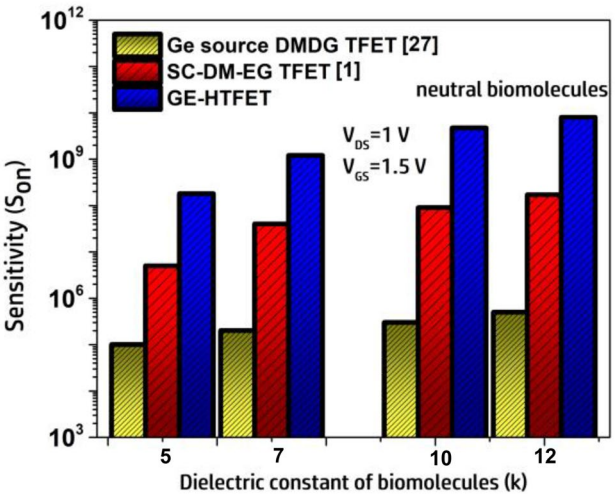

Fig. 14 Comparative study of Ge source DMDG TFET, SC-DM-EG TFET, GE-HTFET on ON current sensitivity

4 Conclusion

The performance of TFET-based biosensor by incorporating the benefits of extended gate architecture and InAs as source material for label-free detection of neutral and charged biomolecules has been studied here. DC and transient analysis of ON current sensitivity has been demonstrated by considering the impact of dielectric constant and charge of biomolecules within the nano-cavity. Results reveal that the sensitivity increases as dielectric constant (k) of bio-species increases from $k=2.1$ to $k=12$ with maximum sensitivity of 7.96×10^{9} for neutral gelatin biomolecule ($k=12$). Likewise, ON current sensitivity increases (decreases) as positive (negative) charge of bio molecules increases for same value of k. Transient response also shows that Ion takes longer time to reach steady state for empty cavity as compared to filled nanogap with shortest settling time being for gelation ($k=12$) and $N=2\times10^{11}\mathrm{Ccm}^{-2}$. Moreover, maximum selectivity (ΔS)~ 10^{2} has been achieved for biotin ($k=2.63$) over streptavidin ($k=2.1$), and minimum selectivity (ΔS)~ 10^{0} is exhibited for gelatin ($k=12$) over keratin ($k=10$). Overall sensitivity is found to be increased when the biomolecules are located at source/channel interface. Finally, high ON state current sensitivity of the GE-HTFET as compared to recently reported structures justifies the implementation of the present structure in developing a highly sensible biomedical tool in future.

Data availability No data was used for the research described in the article.

References

1. S. Mukhopadhyay, D. Sen, B. Goswami, S.K. Sarkar, Performance evaluation of dielectrically modulated extended gate single cavity InGaAs/Si HTFET based label-free biosensor considering non-ideal issues. IEEE Sens. J. **21**(4), 4739–4746 (2020)
2. P. Venkatesh, K. Nigam, S. Pandey, D. Sharma, P.N. Kondekar, A dielectrically modulated electrically doped tunnel FET for application of label free biosensor. Superlattices Microstruct. **109**, 470–479 (2017)
3. N. Bagga, S.K. Sarkar, An analytical model for tunnel barrier modulation in triple metal double gate TFET. IEEE Trans. Electron Devices **62**(7), 2136–2142 (2015)
4. S. Kumar, E. Goel, K. Singh, B. Singh, M. Kumar, S. Jit, A compact 2-D analytical model for electrical characteristics of double-gate tunnel field-effect transistors with a SiO 2/High-$ k $ stacked gate-oxide structure. IEEE Trans. Electron Devices **63**(8), 3291–3299 (2016)
5. D. Sen, P. Saha, S.K. Sarkar, Analysis of dual metal gate engineered SiGe/Si TFET based biosensor: a dielectric modulation approach, in *2021 devices for integrated circuit (DevIC)*. (IEEE, New York, 2021), pp.421–424
6. D.B. Abdi, M.J. Kumar, Controlling ambipolar current in tunneling FETs using overlapping gate-on-drain. IEEE J. Electron Devices Soc. **2**(6), 187–190 (2014)
7. M. Venkatesh, N.B. Balamurugan, New subthreshold performance analysis of germanium based dual halo gate stacked triple material surrounding gate tunnel field effect transistor. Superlattices Microstruct. **130**, 485–498 (2019)
8. S. Chen, S. Wang, H. Liu, T. Han, H. Xie, C. Chong, A novel Dopingless fin-shaped SiGe channel TFET with improved performance. Nanoscale Res. Lett. **15**(1), 1–8 (2020)
9. W.Y. Choi, B.G. Park, J.D. Lee, T.J.K. Liu, Tunneling field-effect transistors (TFETs) with subthreshold swing (SS) less than 60 mV/dec. IEEE Electron Device Lett. **28**(8), 743–745 (2007)
10. S. Kanungo, S. Chattopadhyay, P.S. Gupta, K. Sinha, H. Rahaman, Study and analysis of the effects of SiGe source and pocket-doped channel on sensing performance of dielectrically modulated tunnel FET-based biosensors. IEEE Trans. Electron Devices **63**(6), 2589–2596 (2016)
11. R. Narang, M. Saxena, M. Gupta, Comparative analysis of dielectric-modulated FET and TFET-based biosensor. IEEE Trans. Nanotechnol. **14**(3), 427–435 (2015)
12. V.D. Wangkheirakpam, B. Bhowmick, P.D. Pukhrambam, N+ pocket doped vertical TFET based dielectric-modulated biosensor considering non-ideal hybridization issue: a simulation study. IEEE Trans. Nanotechnol. **19**, 156–162 (2020)
13. S. Kumar, Y. Singh, B. Singh, P.K. Tiwari, Simulation study of dielectric modulated dual channel trench gate TFET-based biosensor. IEEE Sens. J. **20**(21), 12565–12573 (2020)
14. S. Kanungo, B. Majumdar, S. Mukhopadhyay, D. Som, S. Chattopadhyay, H. Rahaman, Investigation on the effects of substrate, back-gate bias and front-gate engineering on the performance of DMTFET-based biosensors. IEEE Sens. J. **20**(18), 10405–10414 (2020)
15. M.R. Tripathy, A.K. Singh, K. Baral, P.K. Singh, S. Jit, III-V/Si staggered heterojunction based source-pocket engineered vertical TFETs for low power applications. Superlattices Microstruct. **142**, 106494 (2020)
16. K.E. Moselund, D. Cutaia, H. Schmid, M. Borg, S. Sant, A. Schenk, H. Riel, Lateral InAs/Si p-type tunnel FETs integrated

on Si—part 1: experimental devices. IEEE Trans. Electron Devices **63**(11), 4233–4239 (2016)
17. K. Vanlalawmpuia, B. Bhowmick, Analysis of hetero-stacked source TFET and heterostructure vertical TFET as dielectrically modulated label-free biosensors. IEEE Sens. J. **22**(1), 939–947 (2021)
18. K. Tomioka, J. Motohisa, S. Hara, T. Fukui, Control of InAs nanowire growth directions on Si. Nano Lett. **8**(10), 3475–3480 (2008)
19. A. Anam, S. Anand, S.I. Amin, Design and performance analysis of tunnel field effect transistor with buried strained Si 1–x Ge x source structure based biosensor for sensitivity enhancement. IEEE Sens. J. **20**(22), 13178–13185 (2020)
20. S.M. Biswal, S.K. Das, S. Misra, U. Nanda, B. Jena, Study on analog/RF and linearity performance of staggered heterojunction gate stack tunnel FET. ECS J. Solid State Sci. Technol. **10**(7), 073001 (2021)
21. ATLAS Device Simulation Software, Silvaco Int., Santa Clara, CA, USA, 2014
22. S. Sant, K. Moselund, D. Cutaia, H. Schmid, M. Borg, H. Riel, A. Schenk, Lateral InAs/Si p-type tunnel FETs integrated on Si—part 2: simulation study of the impact of interface traps. IEEE Trans. Electron Devices **63**(11), 4240–4247 (2016)
23. P. Dwivedi, R. Singh, B.S. Sengar, A. Kumar, V. Garg, A new simulation approach of transient response to enhance the selectivity and sensitivity in tunneling field effect transistor-based biosensor. IEEE Sens. J. **21**(3), 3201–3209 (2020)
24. S.J. Mukhopadhyay, B. Majumdar, K.N. Chappanda, S.C. Mukhopadhyay, S. Kanungo, Performance analysis of the diagonal tunneling-based dielectrically modulated tunnel FET for Biosensing applications. IEEE Sens. J. **21**(19), 21643–21652 (2021)
25. D. Sen, S.D. Patel, S. Sahay, Dielectric modulated nanotube tunnel field-effect transistor as a label free biosensor: proposal and investigation. IEEE Trans. NanoBiosci. (2022). https://doi.org/10.1109/TNB.2022.3172553
26. R. Gautam, M. Saxena, R.S. Gupta, M. Gupta, Gate all around MOSFET with vacuum gate dielectric for improved hot carrier reliability and RF performance. IEEE Trans. Electron Devices **60**(6), 1820–1827 (2013)
27. R. Saha, Y. Hirpara, S. Hoque, Sensitivity analysis on dielectric modulated Ge-source DMDG TFET based label-free biosensor. IEEE Trans. Nanotechnol. **20**, 552–560 (2021)
28. X. Chen, Z. Guo, G.M. Yang, J. Li, M.Q. Li, J.H. Liu, X.J. Huang, Electrical nanogap devices for biosensing. Mater. Today **13**(11), 28–41 (2010)
29. A. Wei, M.J. Sherony, D.A. Antoniadis, Transient behavior of the kink effect in partially-depleted SOI MOSFET's. IEEE Electron Device Lett. **16**(11), 494–496 (1995)
30. A. Gedam, B. Acharya, G.P. Mishra, Design of a double cavity nanotube tunnel field-effect transistor-based biosenser. ECS J. Solid State Sci. Technol. **11**(8), 081012 (2022)
31. P. Dwivedi, R. Singh, Investigation the impact of the gate work-function and biases on the sensing metrics of TFET based biosensors. Eng. Res. Express **2**(2), 025043 (2020)
32. X. Tang, A.M. Jonas, B. Nysten, S. Demoustier-Champagne, F. Blondeau, P.P. Prévot, V. Bayot, Direct protein detection with a nano-interdigitated array gate MOSFET. Biosens. Bioelectron. **24**(12), 3531–3537 (2009)
33. R. Narang, K.S. Reddy, M. Saxena, R.S. Gupta, M. Gupta, A dielectric-modulated tunnel-FET-based biosensor for label-free detection: analytical modeling study and sensitivity analysis. IEEE Trans. Electron Devices **59**(10), 2809–2817 (2012)
34. A. Gao, N. Lu, Y. Wang, T. Li, Robust ultrasensitive tunneling-FET biosensor for point-of-care diagnostics. Sci. Rep. **6**(1), 1–9 (2016)
35. D. Sarkar, K. Banerjee, Proposal for tunnel-field-effect-transistor as ultra-sensitive and label-free biosensors. Appl. Phys. Lett. **100**(14), 143108 (2012)
36. P.R. Nair, M.A. Alam, Design considerations of silicon nanowire biosensors. IEEE Trans. Electron Devices **54**(12), 3400–3408 (2007)
37. C.H. Kim, J.H. Ahn, K.B. Lee, C. Jung, H.G. Park, Y.K. Choi, A new sensing metric to reduce data fluctuations in a nanogap-embedded field-effect transistor biosensor. IEEE Trans. Electron Devices **59**(10), 2825–2831 (2012)
38. Z. Ahangari, Performance assessment of dual material gate dielectric modulated nanowire junctionless MOSFET for ultrasensitive detection of biomolecules. RSC Adv. **6**(92), 89185–89191 (2016)
39. P. Dwivedi, R. Singh, Y.S. Chauhan, Crossing the Nernst limit (59 mV/pH) of sensitivity through tunneling transistor-based biosensor. IEEE Sens. J. **21**(3), 3233–3240 (2020)
40. P. Dwivedi, A. Kranti, Overcoming biomolecule location-dependent sensitivity degradation through point and line tunneling in dielectric modulated biosensors. IEEE Sens. J. **18**(23), 9604–9611 (2018)
41. P. Dwivedi, A. Kranti, Dielectric modulated biosensor architecture: tunneling or accumulation based transistor? IEEE Sens. J. **18**(8), 3228–3235 (2018)
42. M. Verma, S. Tirkey, S. Yadav, D. Sharma, D.S. Yadav, Performance assessment of a novel vertical dielectrically modulated TFET-based biosensor. IEEE Trans. Electron Devices **64**(9), 3841–3848 (2017)
43. S. Shreya, A.H. Khan, N. Kumar, S.I. Amin, S. Anand, Core-shell junctionless nanotube tunnel field effect transistor: design and sensitivity analysis for biosensing application. IEEE Sens. J. **20**(2), 672–679 (2019)
44. S. Anand, A. Singh, S.I. Amin, A.S. Thool, Design and performance analysis of dielectrically modulated doping-less tunnel FET-based label free biosensor. IEEE Sens. J. **19**(12), 4369–4374 (2019)